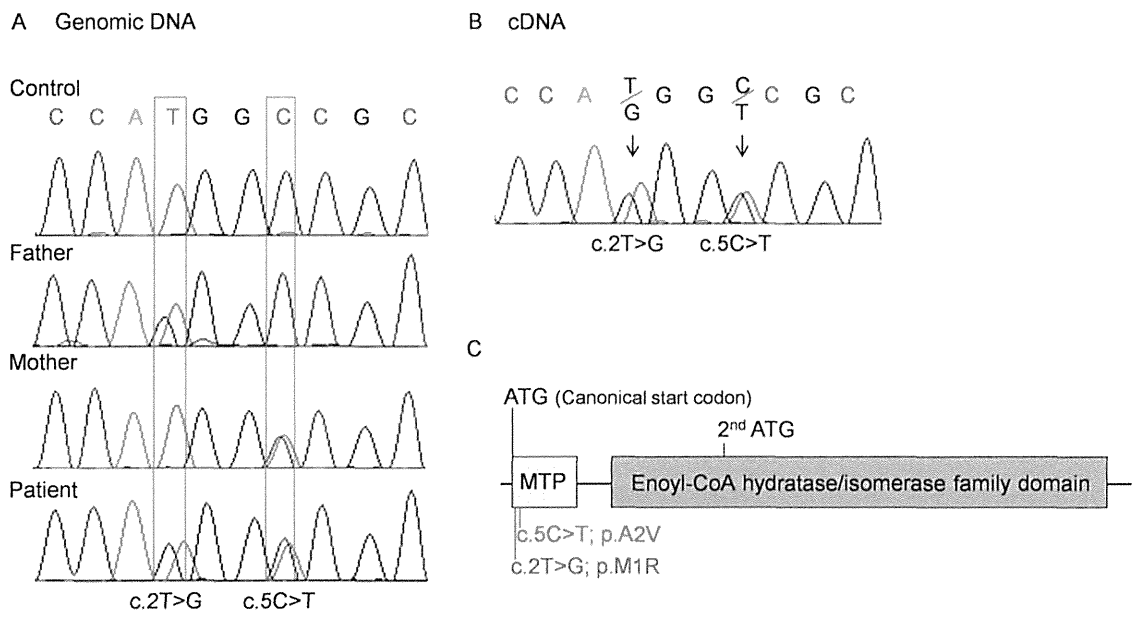

Figure 2. *ECHS1* Sanger sequencing analysis and ECHS1 functional domains. **A**: Sequence chromatograms from part of exon 1 of *ECHS1* were generated by Sanger sequencing of genomic DNA. Each parent had one wild-type allele; the patient's father also harbored a c.2T>G variant, and the patient's mother a c.5C>T variant. The patient inherited each variant allele and was a compound heterozygote. **B**: Sequence chromatograms from part of *ECHS1* exon 1 obtained by Sanger sequencing of cDNA prepared from patient mRNA. The same variants seen in genomic DNA were observed in the cDNA. **C**: A schematic diagram of the functional domains in ECHS1 and the locations of the mutations. MTP, mitochondrial transit peptide.

fractions prepared from patient and control skeletal muscle were used; whole-cell lysates or mitochondrial fractions prepared from patient-derived or control myoblasts were also used. All experiments using these specimens showed that the expression level of ECHS1 protein of the patient was too low to detect by immunoblotting even though the expression level of SDHA was almost the same as controls (Fig. 3A–C). These findings indicated that c.2T>G; p.M1R and c.5C>T; p.A2V mutations caused a remarkable reduction in ECHS1 protein expression. Notably, patient-derived and control myoblasts were similar with regard to *ECHS1* mRNA expression (Fig. 3D), indicating that the mutations apparently affected ECHS1 protein expression directly. Next, we measured ECHS1 enzyme activity in mitochondrial fractions prepared from patient-derived and control myoblasts. ECHS1 activity was normalized to CS activity, and activity in patient-derived myoblasts was 13% of that in control myoblasts (Fig. 3E). Therefore, the mutations caused a severe depletion of ECHS1 protein expression thereby decreasing ECHS1 enzyme activity.

To examine the stability of each mutated protein, we constructed three pIRES2-AcGFP1 expression plasmids, each expressed a different HA-tagged protein: wild-type, M1R-mutant, or A2V-mutant ECHS1. The expression of AcGFP was used as a transfection control. After the transfection into DLD-1 cells, immunoblotting of whole-cell lysate with anti-HA and GFP antibodies showed markedly higher expression of wild-type ECHS1 than of either mutant protein; all ECHS1 expression was normalized to AcGFP expression (Fig. 4, Supp. Fig. S2). This result indicated that ECHS1 protein expression was significantly reduced in the patient because of each mutation.

To confirm that the patient had ECHS1 deficiency, we performed a cellular complementation experiment. Patient-derived myoblasts had to be immortalized for these experiments because nonimmortalized cells exhibited poor growth and finite proliferation. The patient-derived myoblasts and control myoblasts were transfected with pEF321-T vector (a kind gift from Dr. Sumio Sugano, University of Tokyo). We then ascertained that ECHS1 protein expression and activity were lower in immortalized patient-derived myoblasts than in controls (Fig. 5A and B). We then transduced an empty expression vector, pEBMulti-Pur (Wako), or a pEBMulti-Pur construct containing a full-length, wild-type *ECHS1* cDNA into the immortalized patient-derived myoblasts; cells with the vector only or the ECHS1-expression construct are hereafter called vector-only and rescued myoblasts, respectively. ECHS1 protein expression level and enzyme activity were analyzed in mitochondrial fractions prepared from rescued myoblasts. Relative expression level of ECHS1 in rescued myoblasts was 11 times higher than that in vector-only myoblasts (Fig. 5A), and ECHS1 activity normalized to CS activity in rescued myoblasts was 49 times higher than that in vector-only myoblasts (Fig. 5B). From these cellular complementation experiments, we concluded the patient had ECHS1 deficiency.

Since the patient showed the combined mitochondrial respiratory chain deficiency in the skeletal muscle as mentioned above, we used a cellular complementation experiment to determine whether wild-type ECHS1 rescued the respiratory chain defect in patient-derived myoblasts. First, we measured enzyme activities of each mitochondrial respiratory complex in mitochondrial fractions prepared from immortalized patient-derived myoblasts. CS activity normalized values for complexes I, IV, and V activity in immortalized patient-derived myoblasts were decreased to 17%, 39%, and 43% of the mean values of immortalized control myoblasts (Fig. 5C). Then, we measured enzyme activity in mitochondrial fractions prepared from rescued myoblasts and found that each activity of complexes I, IV, and V was mostly restored relative to that in vector-only myoblasts. In rescued myoblasts, CS activity normalized values of complexes I, IV, and V were 3.5, 1.3, and 2.2 times higher than those in vector-only myoblasts (Fig. 5C). Mitochondrial respiratory complex activity was mostly restored in rescued myoblasts, suggesting that there was an unidentified link between deficiency of ECHS1 and respiratory chain.

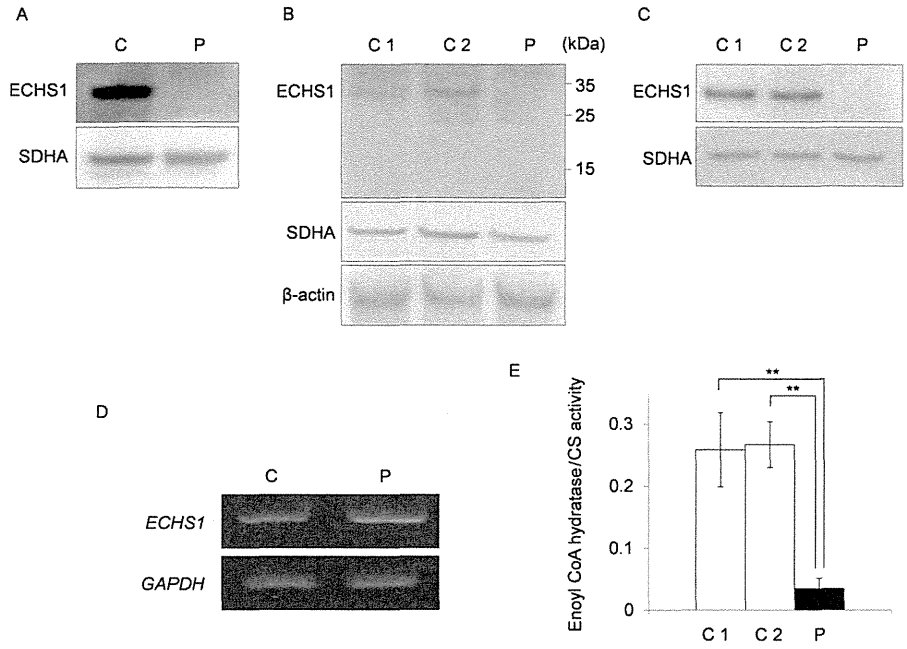

Figure 3. ECHS1 expression and enzyme activity. ECHS1 expression was analyzed by immunoblotting. C1/2, control; P, patient. Mitochondrial fraction prepared from patient's skeletal muscle (**A**) or whole-cell lysate (**B**) and mitochondrial fraction (**C**) prepared from the patient-derived myoblasts were analyzed via immunoblotting. All findings indicated that ECHS1 levels in patient samples were too low to detect by immunoblotting. **D**: RT-PCR was used to assess *ECHS1* mRNA levels in the patient. Notably, patient-derived myoblasts and control myoblasts did not differ with regard to *ECHS1* mRNA level. **E**: Mitochondrial fractions prepared from patient-derived myoblasts were used to estimate ECHS1 enzyme activity in the patient. All ECHS1 activity measurements were normalized to CS activity; ECHS1 activity in patient-derived samples was 13% of that in control samples. The experiments were performed in triplicate. Error bars represent standard deviations. (** $P < 0.005$ Student's *t*-test).

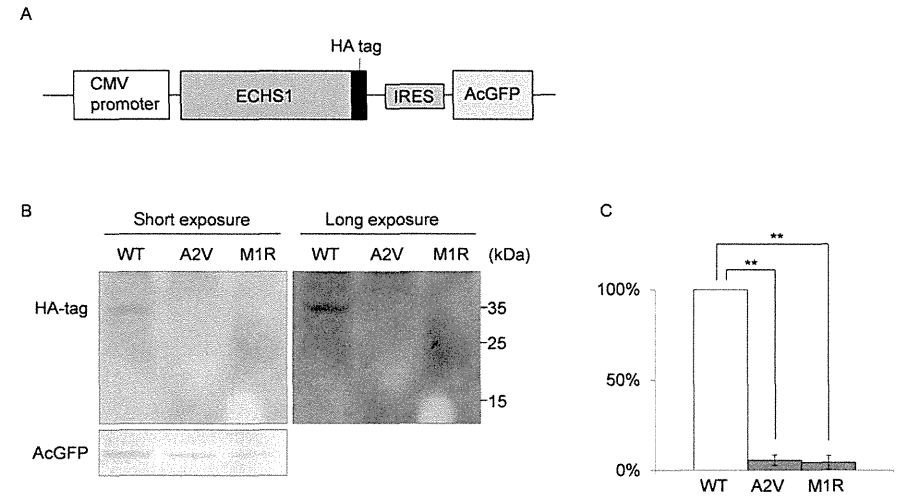

Figure 4. Exogenous expression of mutant ECHS1 protein in cancer cells. **A**: Schematic diagram of the pIRES mammalian expression vector. **B**: Representative image of an immunoblotting containing AcGFP, an internal control, and each HA-tagged ECHS1 protein; all proteins were isolated from DLD-1 cells that transiently overexpressed wild-type, A2V, or M1R HA-tagged ECHS1 from pIRES. The images obtained by short exposure (left) and long exposure (right). **C**: Overexpressed HA-tagged ECHS1 protein levels. Both mutant ECHS1 proteins showed dramatically decreased expression compared to wild-type ECHS1 protein, when ECHS1 was normalized relative to the internal control. Each experiment was performed in triplicate. Error bars represent standard deviations (** $P < 0.005$ Student's *t*-test).

Discussion

Here, we described a patient harboring compound heterozygous mutations in *ECHS1*. Immunoblotting analysis revealed that ECHS1 protein was undetectable in patient-derived myoblasts; moreover, these cells showed significantly lower ECHS1 enzyme activity than controls. Exogenous expression of two recombinant mutant proteins in DLD-1 cells showed c.2T>G; p.M1R and c.5C>T; p.A2V mutations affected ECHS1 protein expression. Cellular complementation experiment verified the patient had ECHS1 deficiency.

The c.2T>G; p.M1R mutation affected the start codon and therefore was predicted to impair the protein synthesis from canonical

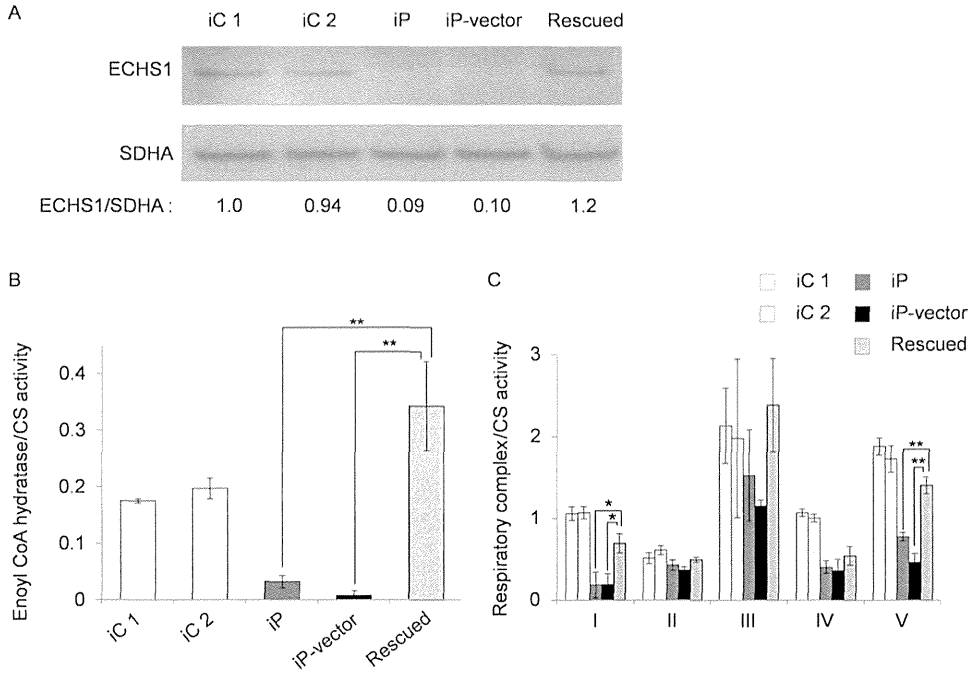

Figure 5. ECHS1 protein expression and enzyme activity in rescued myoblasts. An empty vector or a construct encoding wild-type ECHS1 was introduced into immortalized patient-derived myoblasts. iC1/2, immortalized control myoblasts; iP, immortalized patient-derived myoblasts; iP-vector, immortalized patient-derived myoblasts transfected with empty vector; Rescued, immortalized patient-derived myoblasts stably expressing wild-type ECHS1. **A**: ECHS1 levels were assessed on immunoblotting using mitochondrial fractions prepared from rescued myoblasts. ECHS1 level in "rescued" is 11 times higher than that in "iP-vector". **B**: Mitochondrial fractions prepared from rescued myoblasts were also used to measure ECHS1 enzyme activity. ECHS1 activity normalized to CS activity in "rescued" was 49 times higher than that in "iP-vector." Each experiment was performed in triplicate. Error bars represent standard deviations (** $P < 0.005$ Student's *t*-test). **C**: Mitochondrial fractions prepared from rescued myoblasts were used to measure enzyme activities of mitochondrial respiratory complexes. Activity values were normalized to CS activity. Activities of complexes I, IV, and V were mostly restored from "iP" and "iP-vector." In "rescued," the enzyme activities of complexes I, IV, and V were 3.5, 1.3, and 2.2 times higher, respectively, than the "iP-vector." Each experiment was performed in triplicate. Error bars represent standard deviations (** $P < 0.005$, * $P < 0.05$ Student's *t*-test).

initiation site. In the reference *ECHS1* sequence, the next in-frame start codon is located in amino acids 97 (Fig. 2C). Even if translation could occur from this second start codon, the resulting product would lack the whole transit peptide and part of the enoyl-CoA hydratase/isomerase family domain (Fig. 2C). The c.5C>T; p.A2V mutation was located in the mitochondrial transit peptide and the mutation may affect the mitochondrial translocation of ECHS1. Surprisingly, the MitoProt-predicted mitochondrial targeting scores for the wild-type and A2V-mutant proteins were 0.988 and 0.991, respectively [MitoProt II; http://ihg.gsf.de/ihg/mitoprot.html; Claros and Vincens, 1996] and not markedly different from each other. Nevertheless, mislocalized mutant protein may have been degraded outside of the mitochondria. Consistent with this speculation was the finding that immunoblotting of lysate from patient-derived myoblasts (Fig. 3B) or from transfected cells that overexpressed the recombinant p.A2V-mutant ECHS1 (Fig. 4B, Supp. Fig. S2) did not show upper shifted ECHS1 bands that indicated ECHS1 with the transit peptide. Another possible explanation is that the mutation affected the translation efficiency because it was very close to the canonical start codon. It can change secondary structure of ECHS1 mRNA or alter the recognition by the translation initiation factors. As stated above, even if there was a translation product from the second in-frame start codon, that product would probably not function.

This patient presented with symptoms that are indicative of fatty acid oxidation disorders (e.g., hypotonia and metabolic acidosis), but he also presented with neurologic manifestations, including developmental delay and Leigh syndrome, that are not normally associated with fatty acid β-oxidation disorders. Interestingly, developmental delay is also found in cases of SCAD deficiency [Jethva et al., 2008]. In the absence of SCAD, the byproducts of butyryl-CoA—including butyrylcarnitine, butyrylglycine, ethylmalonic acid (EMA), and methylsuccinic acid—accumulate in blood, urine, and cells. These byproducts may cause the neurological pathology associated with SCAD deficiency [Jethva et al., 2008]. EMA significantly inhibits creatine kinase activity in the cerebral cortex of Wistar rats but does not affect levels in skeletal or heart muscle [Corydon et al., 1996]. Elevated levels of butyric acid modulated gene expression because excess butyric acid can enhance histone deacetylase activity [Chen et al., 2003]. Moreover, the highly volatile nature of butyric acid as a free acid may also add to its neurotoxic effects [Jethva et al., 2008].

On the other hand, it is very rare for fatty acid β-oxidation disorders causing Leigh syndrome. Therefore, the most noteworthy manifestation in this patient was Leigh syndrome. Leigh syndrome is a neuropathological entity characterized by symmetrical necrotic lesions along the brainstem, diencephalon, and basal ganglion [Leigh, 1951]. It is caused by abnormalities of mitochondrial energy generation and exhibits considerable clinical and genetic heterogeneity [Chol et al., 2003]. Commonly, defects in the mitochondrial respiratory chain or the pyruvate dehydrogenase complex are responsible for this disease. This patient's skeletal muscle samples exhibited a combined respiratory chain deficiency, and this deficiency may be the reason that he presented with Leigh syndrome. Although it

remained unclear what caused the respiratory chain defect, cellular complementation experiments showed almost complete restoration, indicating there was an unidentified link between ECHS1 and respiratory chain. One of the possible causes of respiratory chain defect is the secondary effect of accumulation of toxic metabolites. For example, an elevated urine glyoxylate was observed in this patient. Although the mechanism of this abnormal accumulation is not clear at the moment, it was shown that glyoxylate inhibited oxidative phosphorylation or pyruvate dehydrogenase complex by in vitro systems [Whitehouse et al., 1974; Lucas and Pons, 1975]. Therefore, we speculate that in our patient, ECHS1 deficiency induced metabolism abnormality including glyoxylate accumulation, and glyoxylate played a role in decreased enzyme activities of respiratory chain complexes. Interestingly, a recent paper describing patients with Leigh syndrome and ECHS1 deficiency showed decreased activity of pyruvate dehydrogenase complex in fibroblasts [Peters et al., 2014], (Supp. Table S5). BN-PAGE showed the assembly of respiratory complex components in the patient was not clearly different from the control (Supp. Fig. S1). This result suggests that the respiratory chain defect in the patient is more likely because of the secondary effect of accumulation of toxic metabolites. On the other hand, many findings indicate interplays between mitochondrial fatty acid β-oxidation and the respiratory chain. For example, Enns et al. [2000] mentioned the possibility of the physical association between these two energy-generating pathways from overlapping clinical phenotypes in genetic deficiency states. More recently, Wang and his colleagues actually showed physical association between mitochondrial fatty acid β-oxidation enzymes and respiratory chain complexes (Wang et al., 2010). Similarly, Narayan et al. demonstrated interactions between short-chain 3-hydroxyacyl-CoA dehydrogenase (SCHAD) and several components of the respiratory chain complexes including the catalytic subunits of complexes I, II, III, and IV via pull-down assays involving several mouse tissues. Considering the role of SCHAD as a NADH-generating enzyme, this interaction was suggested to demonstrate the logical physical association with the regeneration of NAD through the respiratory chain [Narayan et al., 2012]. Still more recently, mitochondrial protein acetylation was found to be driven by acetyl-CoA produced from mitochondrial fatty acid β-oxidation [Pougovkina et al., 2014]. Because the activities of respiratory chain enzymes are regulated by protein acetylation [Zhang et al., 2012], this finding indicated that β-oxidation regulates the mitochondrial respiratory chain. Remarkably, acyl-CoA dehydrogenase 9 (ACAD9), which participates in the oxidation of unsaturated fatty acid, was recently identified as a factor involved in complex I biogenesis [Haack et al., 2010; Heide et al., 2012]. Cellular complementation experiments that involve overexpression of wild-type ACAD9 in patient-derived fibroblast cell lines showed restoration of complex I assembly and activity [Haack et al., 2010]. Accumulating evidence indicates that there are complex regulatory interactions between mitochondrial fatty acid β-oxidation and the respiratory chain.

ECHS1 has been shown to interact with several molecules outside the mitochondrial fatty acid β-oxidation pathway [Chang et al., 2013; Xiao et al., 2013] and the loss of this interaction can affect respiratory chain function in a patient. Further functional analysis of ECHS1 will advance our understanding of the complex regulation of mitochondrial metabolism.

Acknowledgments

We acknowledge the technical support of Dr. Ichizo Nishino, Dr. Ikuya Nonaka, Dr. Chikako Waga, Takao Uchiumi, Yoshie Sawano, and Michiyo Nakamura. We also thank Dr. Sumio Sugano (the University of Tokyo) for providing the pEF321-T plasmid.

Disclosure statement: The authors have no conflict of interest to declare.

References

Chang Y, Wang SX, Wang YB, Zhou J, Li WH, Wang N, Fang DF, Li HY, Li AL, Zhang XM, Zhang WN. 2013. ECHS1 interacts with STAT3 and negatively regulates STAT3 signaling. FEBS Lett 587:607–613.

Chen JS, Faller DV, Spanjaard RA. 2003. Short-chain fatty acid inhibitors of histone deacetylases: promising anticancer therapeutics? Curr Cancer Drug Targets 3:219–236.

Chol M, Lebon S, Bénit P, Chretien D, de Lonlay P, Goldenberg A, Odent S, Hertz-Pannier L, Vincent-Delorme C, Cormier-Daire V, Rustin P, Rötig A, et al. 2003. The mitochondrial DNA G13513A MELAS mutation in the NADH dehydrogenase 5 gene is a frequent cause of Leigh-like syndrome with isolated complex I deficiency. J Med Genet 40:188–191.

Claros MG, Vincens P. 1996. Computational method to predict mitochondrially imported proteins and their targeting sequences. Eur J Biochem 241:779–786.

Corydon MJ, Gregersen N, Lehnert W, Ribes A, Rinaldo P, Kmoch S, Christensen E, Kristensen TJ, Andresen BS, Bross P, Winter V, Martinez G, et al. 1996. Ethylmalonic aciduria is associated with an amino acid variant of short chain acyl-coenzyme A dehydrogenase. Pediatr Res 39:1059–1066.

Enns GM, Bennett MJ, Hoppel CL, Goodman SI, Weisiger K, Ohnstad C, Golabi M, Packman S. 2000. Mitochondrial respiratory chain complex I deficiency with clinical and biochemical features of long-chain 3-hydroxyacyl-coenzyme A dehydrogenase deficiency. J Pediatr 136:251–254.

Ensenauer R, He M, Willard JM, Goetzman ES, Corydon TJ, Vandahl BB, Mohsen A-W, Isaya G, Vockley J. 2005. Human acyl-CoA dehydrogenase-9 plays a novel role in the mitochondrial beta-oxidation of unsaturated fatty acids. J Biol Chem 280:32309–32016.

Frezza C, Cipolat S, Scorrano L. 2007. Organelle isolation: functional mitochondria from mouse liver, muscle and cultured filroblasts. Nat Protoc 2:287–295.

Haack TB, Danhauser K, Haberberger B, Hoser J, Strecker V, Boehm D, Uziel G, Lamantea E, Invernizzi F, Poulton J, Rolinski B, Iuso A, et al. 2010. Exome sequencing identifies ACAD9 mutations as a cause of complex I deficiency. Nat Genet 42:1131–1134.

Heide H, Bleier L, Steger M, Ackermann J, Dröse S, Schwamb B, Zörnig M, Reichert AS, Koch I, Wittig I, Brandt U. 2012. Complexome profiling identifies TMEM126B as a component of the mitochondrial complex I assembly complex. Cell Metab 6:538–549.

Hochstrasser DF, Frutiger S, Paquet N, Bairoch A, Ravier F, Pasquali C, Sanchez JC, Tissot JD, Bjellqvist B, Vargas R, Ron DA, Graham JH. 1992. Human liver protein map: a reference database established by microsequencing and gel comparison. Electrophoresis 13:992–1001.

Ikeda Y, Dabrowski C, Tanaka K. 1983. Separation and properties of five distinct acyl-CoA dehydrogenases from rat liver mitochondria. J Biol Chem 258:1066–1076.

Ikeda Y, Hine DG, Okamura-Ikeda K, Tanaka K. 1985a. Mechanism of action of short-chain, medium chain and long-chain acyl-CoA dehydrogenases: direct evidence for carbanion formation as an intermediate step using enzyme-catalyzed C-2 proton/deuteron exchange in the absence of C-3 exchange. J Biol Chem 260: 1326–1337.

Ikeda Y, Okamura-Ikeda K, Tanaka K. 1985b. Spectroscopic analysis of the interaction of rat liver short chain, medium chain and long chain acyl-CoA dehydrogenases with acyl-CoA substrates. Biochemistry 24:7192–7199.

Jethva R, Bennett MJ, Vockley J. 2008. Short-chain acyl-coenzyme A dehydrogenase deficiency. Mol Genet Metab 95:195–200.

Kamijo T, Aoyama T, Miyazaki J, Hashimoto T. 1993. Molecular cloning of the cDNAs for the subunits of rat mitochondrial fatty acid beta-oxidation multienzyme complex. Structural and functional relationships to other mitochondrial and peroxisomal beta-oxidation enzymes. J Biol Chem 268:26452–26460.

Kim DW, Uetsuki T, Kaziro Y, Yamaguchi N, Sugano S. 1990. Use of the human elongation factor 1 alpha promoter as a versatile and efficient expression system. Gene 91:217–223.

Kompare M, Rizzo WB. 2008. Mitochondrial fatty-acid oxidation disorders. Semin Pediatr Neurol 15:140–149.

Leigh D. 1951. Subacute necrotizing encephalomyelopathy in an infant. J Neurol Neurosurg Psychiatr 14:216–221.

Lucas M, Pons AM. 1975. Influence of glyoxylic acid on properties of isolated mitochondria. Biochimie 57:637–645.

Matsunaga T, Kumanomido H, Shiroma M, Goto Y, Usami S. 2005. Audiological features and mitochondrial DNA sequence in a large family carrying mitochondrial A1555G mutation without use of aminoglycoside. Ann Otol Rhinol Laryngol 114:153–160.

Morava E, Rodenburg RJ, Hol F, de Vries M, Janssen A, van den Heuvel L, Nijtmans L, Smeitink J. 2006. Clinical and biochemical characteristics in patients with a high mutant load of the mitochondrial T8993G/C mutations. Am J Med Genet A 140:863–868.

Narayan, SB, Master SR, Sirec AN, Bierl C, Stanley PE, Li C, Stanley CA, Bennett MJ. 2012. Short-chain 3-hydroxyacyl-coenzyme A dehydrogenase associates with a protein super-complex integrating multiple metabolic pathways. PLoS One 7: e35048.

Peters H, Buck N, Wanders R, Ruiter J, Waterham H, Koster J, Yaplito-Lee J, Ferdinandusse S, Pitt J. 2014. ECHS1 mutations in Leigh disease: a new inborn error of metabolism affecting valine metabolism. Brain 137: 2903–2908.

Pougovkina O, Te Brinke H, Ofman R, van Cruchten AG, Kulik W, Wanders RJ, Houten SM, de Boer VC. 2014. Mitochondrial protein acetylation is driven by acetyl-CoA from fatty acid oxidation. Hum Mol Genet 23:3513–3522.

Shimazaki H, Takiyama Y, Ishiura H, Sakai C, Matsushima Y, Hatakeyama H, Honda J, Sakoe K, Naoi T, Namekawa M, Fukuda Y, Takahashi Y, et al. 2012. A homozygous mutation of C12orf65 causes spastic paraplegia with optic atrophy and neuropathy (SPG55). J Med Genet 49:777–784.

Spiekerkoetter U, Khuchua Z, Yue Z, Bennett MJ, Strauss AW. 2004. General mitochondrial trifunctional protein (TFP) deficiency as a result of either alpha- or beta-subunit mutations exhibits similar phenotypes because mutations in either subunit alter TFP complex expression and subunit turnover. Pediatr Res 55:190–196.

Steinman HM, Hill RL. 1975. Bovine liver crotonase (enoyl coenzyme A hydratase). Methods Enzymol 35:136–151.

Uchida Y, Izai K, Orii T, Hashimoto T. 1992. Novel fatty acid beta-oxidation enzymes in rat liver mitochondria. II. Purification and properties of enoyl-coenzyme A (CoA) hydratase/3-hydroxyacyl-CoA dehydrogenase/3-ketoacyl-CoA thiolase trifunctional protein. J Biol Chem 267:1034–1041.

Wang Y, Mohsen AW, Mihalik SJ, Goetzman ES, Vockley J. 2010. Evidence for physical association of mitochondrial fatty acid oxidation and oxidative phosphorylation complexes. J Biol Chem 285:29834–29841.

Whitehouse S, Cooper RH, Randle PJ. 1974. Mechanism of activation of pyruvate dehydrogenase by dichloroacetate and other halogenated carboxylic acids. Biochem J 141:761–774.

Xiao CX, Yang XN, Huang QW, Zhang YQ, Lin BY, Liu JJ, Liu YP, Jazag A, Guleng B, Ren JL. 2013. ECHS1 acts as a novel HBsAg-binding protein enhancing apoptosis through the mitochondrial pathway in HepG2 cells. Cancer Lett 330:67–73.

Zhang J, Lin A, Powers J, Lam MP, Lotz C, Liem D, Lau E, Wang D, Deng N, Korge P, Zong, NC, Cai H, et al. 2012. Perspectives on: SGP symposium on mitochondrial physiology and medicine: mitochondrial proteome design: from molecular identity to pathophysiological regulation. J Gen Physiol 139:395–406.

Hum Genet (2014) 133:225–234
DOI 10.1007/s00439-013-1372-6

ORIGINAL INVESTIGATION

A hemizygous *GYG2* mutation and Leigh syndrome: a possible link?

Eri Imagawa · Hitoshi Osaka · Akio Yamashita · Masaaki Shiina · Eihiko Takahashi · Hideo Sugie · Mitsuko Nakashima · Yoshinori Tsurusaki · Hirotomo Saitsu · Kazuhiro Ogata · Naomichi Matsumoto · Noriko Miyake

Received: 17 April 2013 / Accepted: 29 September 2013 / Published online: 8 October 2013

Abstract Leigh syndrome (LS) is an early-onset progressive neurodegenerative disorder characterized by unique, bilateral neuropathological findings in brainstem, basal ganglia, cerebellum and spinal cord. LS is genetically heterogeneous, with the majority of the causative genes affecting mitochondrial malfunction, and many cases still remain unsolved. Here, we report male sibs affected with LS showing ketonemia, but no marked elevation of lactate and pyruvate. To identify their genetic cause, we performed whole exome sequencing. Candidate variants were narrowed down based on autosomal recessive and X-linked recessive models. Only one hemizygous missense mutation (c.665G>C, p.W222S) in glycogenin-2 (*GYG2*) (isoform a: NM_001079855) in both affected sibs and a heterozygous change in their mother were identified, being consistent with the X-linked recessive trait. *GYG2* encodes glycogenin-2 (GYG2) protein, which plays an important role in the initiation of glycogen synthesis. Based on the structural modeling, the mutation can destabilize the structure and result in protein malfunctioning. Furthermore, in vitro experiments showed mutant GYG2 was unable to undergo the self-glucosylation, which is observed in wild-type GYG2. This is the first report of *GYG2* mutation in human, implying a possible link between GYG2 abnormality and LS.

Introduction

Glycogen is a large branched polysaccharide containing linear chains of glucose residues. Glycogen deposits in skeletal muscle and liver serve as shorter-term energy storage in mammals, while fat provides long-term storage. Glycogen biosynthesis begins with self-glucosylation of glycogenins by covalent binding of UDP-glucose to tyrosine residues of the glycogenins and the subsequent extension of approximately ten glucose residues (Pitcher et al. 1988; Smythe et al. 1988). Glycogen particles are formed by the continued addition of UDP-glucose to the growing

Electronic supplementary material The online version of this article (doi:10.1007/s00439-013-1372-6) contains supplementary material, which is available to authorized users.

E. Imagawa · M. Nakashima · Y. Tsurusaki · H. Saitsu · N. Matsumoto (✉) · N. Miyake (✉)
Department of Human Genetics, Yokohama City University Graduate School of Medicine, Yokohama 236-0004, Japan
e-mail: naomat@yokohama-cu.ac.jp

N. Miyake
e-mail: nmiyake@yokohama-cu.ac.jp

H. Osaka
Division of Neurology, Clinical Research Institute, Kanagawa Children's Medical Center, Yokohama 232-8555, Japan

A. Yamashita
Department of Molecular Biology, Yokohama City University School of Medicine, Yokohama 236-0004, Japan

M. Shiina · K. Ogata
Department of Biochemistry, Yokohama City University Graduate School of Medicine, Yokohama 236-0004, Japan

E. Takahashi
Division of Infection and Immunology, Clinical Research Institute, Kanagawa Children's Medical Center, Yokohama 232-8555, Japan

H. Sugie
Department of Pediatrics, Jichi Medical University, Tochigi 329-0498, Japan

glycogen chain by glycogen synthase, and introduction of branches every 10–14 residues by the glycogen branching enzyme (Krisman and Barengo 1975; Larner 1953). To date, two glycogenin paralogues have been identified in human, glycogenin-1 (GYG1) and glycogenin-2 (GYG2). These proteins have been shown to form homodimers, heterodimers and larger oligomers (Gibbons et al. 2002). GYG1 (muscle form) is expressed predominantly in muscle while GYG2 (liver form) is expressed mainly in liver, heart and pancreas (Barbetti et al. 1996; Mu et al. 1997). Biallelic GYG1 abnormality is known to cause muscle weakness and cardiac arrhythmia in humans through GYG1 autoglucosylation failure (Moslemi et al. 2010). However, human disease due to GYG2 abnormality has never been reported.

Leigh syndrome (LS; MIM #256000) was first described as a subacute necrotizing encephalomyelopathy by Dr. Denis Leigh in 1951 (Leigh 1951). LS is a progressive neurodegenerative disorder with an estimated incidence of 1:40,000 live births (Rahman et al. 1996). Onset is usually in early childhood (typically before age 2) (Naess et al. 2009; Ostergaard et al. 2007). Clinical manifestations of LS are observed in the central nervous system (CNS) (developmental delay, hypotonia, ataxia, convulsion, nystagmus, respiratory failure and dysphagia), peripheral nervous system (polyneuropathy and myopathy) and extraneural organs (deafness, diabetes, cardiomyopathy, kidney malfunction and others) (Finsterer 2008). The neurological features depend on the affected regions and degree of severity. The presence of bilateral, symmetrical, focal hyperintense T2-weighted MRI signals in basal ganglia (mainly putamen), thalamus, substantia nigra, substantia ruber, brainstem, cerebellum, cerebral white matter or spinal cord is diagnostic of LS (Farina et al. 2002; Medina et al. 1990). Neuropathological studies revealed that these lesions reflect neuronal necrosis, gliosis and vascular proliferation (Brown and Squier 1996; Leigh 1951). In the majority of LS cases, lactate, pyruvate or the lactate/pyruvate ratio is increased in blood and cerebrospinal fluid (Finsterer 2008). To the best of our knowledge, 37 nuclear genes are known to be mutated in LS, in addition to some mitochondrial genes (Antonicka et al. 2010; Debray et al. 2011; Finsterer 2008; Lopez et al. 2006; Martin et al. 2005; Quinonez et al. 2013). Thus, inheritance patterns of LS include mitochondrial, autosomal recessive and X-linked recessive modes (Benke et al. 1982; van Erven et al. 1987).

We encountered a Japanese family with affected brothers showing atypical LS without marked elevation of lactic or pyruvic acid and unknown etiology. A unique genetic variant was identified by whole exome sequencing (WES), which may be associated with atypical LS phenotype in this family.

Materials and methods

Subjects

Peripheral blood samples of affected brothers diagnosed with LS and their parents were collected after obtaining written informed consent. DNA was extracted from peripheral blood leukocytes using QuickGene-610L (Fujifilm, Tokyo, Japan) according to the manufacturer's instructions. Lymphoblastoid cell lines derived from all family members were established. The Institutional Review Boards of Yokohama City University School of Medicine approved this study.

Causative gene identification

Whole exome sequencing was performed in two affected individuals (II-2 and II-3 in Fig. 1a) as described in the Supplementary methods. All candidate variants based on autosomal and X-linked recessive models were checked by Sanger sequencing in the parents and affected siblings. PCR products amplified with genomic DNA as a template were sequenced on an ABI3500xl autosequencer (Applied Biosystems, Foster City, CA) and analyzed using Sequencher 5.0 (Gene Codes Corporation, Ann Arbor, MI). As the pedigree tree might also indicate mitochondrial inheritance of this disease and LS is known to be caused by mitochondrial genome mutations, we screened the entire mitochondrial genome by the algorithm reported previously (Picardi and Pesole 2012), using exome data (detailed in Supplementary methods).

Structure modeling

To evaluate the effect of the GYG2 missense mutation (c.665G>C, p.W222S in isoform a: NM_001079855) on its function at the molecular structural level, the mutated molecular structure was constructed, and the free energy change caused by the mutation was calculated using the FoldX software (version 3.0) (Guerois et al. 2002; Khan and Vihinen 2010). As crystal structure of human GYG2 is unavailable, that of human GYG1 (Protein Data Bank code; 3T7O) was used as a structural model. The mutation was introduced into one subunit of the GYG1 homodimer. The ligands included in the crystal structure of GYG1 were ignored in the calculation, because the FoldX energy function could not deal with the ligands. The calculation was repeated three times, and the resultant data were presented as an average value with standard deviations.

Preparation for mammalian expression vectors

Human glycogenin-2 isoform a cDNA clone (IMAGE Clone ID: 100008747) integrated in pENTR221 was purchased from Kazusa DNA Research Institute (Chiba, Japan). The

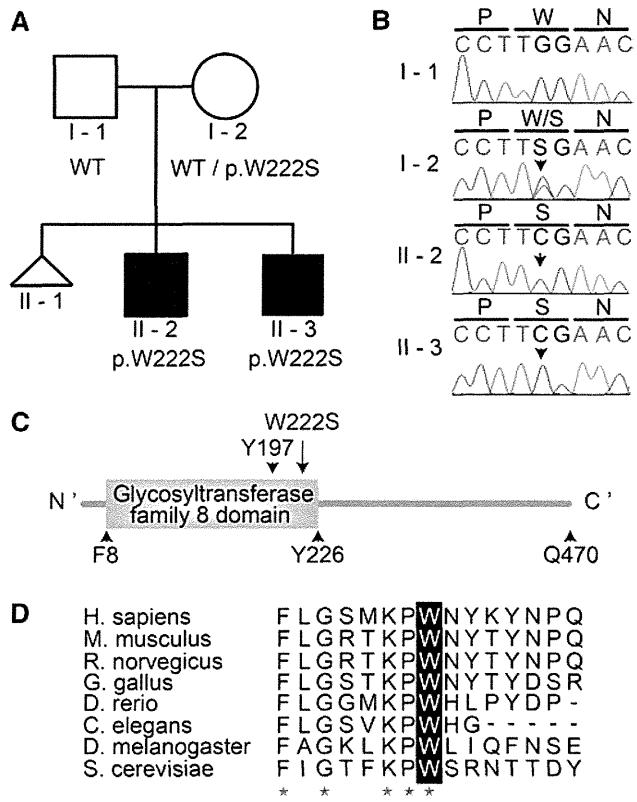

Fig. 1 Mutation Analysis of *GYG2*. **a** Pedigree of the family with a unique type of LS and a *GYG2* mutation (c.665G>C, p.W222S). *Square*, *circle* and *triangle* denote male, female and spontaneous abortion, respectively. *White* and *black symbols* indicate unaffected and affected individuals, respectively, while the affection status of the spontaneous abortion is unknown. **b** Electropherograms of a *GYG2* mutation. **c** The functional domain of human GYG2 (isoform a). The substitution of p.W222S is located within the glycosyltransferase family 8 domain (*yellow square*). **d** The evolutionary conservation of the W222 in GYG2. *Red stars* indicate identical amino acids from *S. cerevisiae* to *H. sapiens*. Sequences were aligned using CLUSTALW (http://www.genome.jp/tools/clustalw/)

missense mutation (c.665G>C, p.W222S) was introduced by Site-directed mutagenesis using the QuikChange II XL site-directed mutagenesis kit (Agilent Technologies, Santa Clara, CA). Wild-type and mutant C' V5/6xHis tagged GYG2 constructs were created using pcDNA-DEST40 (Invitrogen, Carlsbad, CA) by LR recombination in Gateway system (Invitrogen). To create the untagged construct, the last codon was altered to a stop codon by mutagenesis.

Self-glucosylation analysis

Glucosyltransferase activity of GYG2 was measured as previously described (Lomako et al. 1988), with slight modifications. In brief, COS-1 cells were maintained in Dulbecco's modified Eagle's medium (DMEM) (Sigma-Aldrich, Schnelldorf, Germany) containing 10 % heat-inactivated fetal bovine serum (FBS) (Gibco-BRL, Grand Island, NY), 2 mM L-glutamine (Sigma-Aldrich) and 1 % penicillin–streptomycin (Sigma-Aldrich). As previously described (Mu and Roach 1998), the ~80 % confluent COS-1 cells (~1 × 10^7) were transiently transfected by X-treamGENE9 DNA transfection reagent (Roche Applied Science, Foster City, CA) with 5 μg of either a wild-type Human GYG2 (isoform a) expressing plasmid or the same plasmid into which the W222S encoding mutation had been introduced. After 24 h, the cells were collected and lysed in 300 μl of buffer consisting of 50 mM HEPES, 0.5 % Triton X-100, 1 × EDTA-free protease Inhibitor Cocktail tablets (Roche Applied Science), 1 × phosphatase inhibitor cocktail (Nacalai Tesque Inc., Kyoto, Japan) and 0.5 mM β-mercaptoethanol (Mu et al. 1997). After centrifugation at 14,000 rpm for 15 min, 10 μl of the soluble fractions were mixed with 10 μl of 2 × reaction buffer containing 100 mM HEPES (pH7.5), 10 mM MgCl, 4 mM dithiothreitol (DTT) and 40 μM UDP-[^{14}C]-glucose (250 mCi/mmol; PerkinElmer, Waltham, MA) (Cao et al. 1993). After incubation at 30 °C for 30 min, the reaction was stopped by addition of 20 μl of 2 × Laemmli sample buffer (Sigma-Aldrich) (Viskupic et al. 1992). 15 μl of each sample was subjected to SDS-polyacrylamide gel electrophoresis. After treatment with Gel drying solution (Bio-Rad Laboratories, Hercules, CA) for 30 min, gels were dried. Dried gels were then exposed on X-ray film for 2 weeks to detect the incorporation of UDP-[^{14}C]-glucose into GYG2. In addition, the ^{14}C-signal intensities were evaluated using an imaging analyzer, BAS2500 (Fujifilm). Three independent experiments were performed.

Western blot analysis

For the detection of GYG2 protein, rabbit polyclonal anti-GYG2 antibodies (1:500 dilution; Abcam Inc., Cat.#HPA005495, Cambridge, MA) and horse-radish peroxidase (HRP)-conjugated anti-rabbit IgG (1:10,000 dilution; Jackson ImmunoResearch, Cat.#111-035-003, West Grove, PA) were used. Immunoblot chemiluminescence was performed using SuperSignal West Dura as substrate (Thermo Fisher Scientific, Waltham, MA). The chemiluminescence signal images were captured by FluorChem 8900 (Alpha Innotech, San Leandro, CA). Signal intensities were measured by AlphaEase FC (Alpha Innotech). Three independent experiments were performed.

Results

Clinical finding

Patient II-2 (Fig. 1a; Table 1) is a 26-year-old male born to non-consanguineous parents. His mother previously had a

Table 1 Clinical features of the presenting patients affected with LS

	II-2	II-3
Sex	M	M
Age (years)	26	19
Common clinical phenotype		
Psychomotor retardation	+	+
Failure to thrive	+	+
Swallowing difficulties	–	–
Spasticity	+	+
Rigidity	+	+
Pathological reflexes	+	+
Ataxia	+	+
Athetoid movements	+	+
Convulsions	+	+
Ophthalmoplegia	+	+
Strabismus	+	+
Gastrointestinal problems	+	+
Renal agenesis	NA	+
Pes equinovarus	+	+
Uncommon clinical phenotype		
Increase of ketone body	+	+

NA not assessed

spontaneous abortion. He was born at 39 weeks gestation without asphyxia after an uneventful pregnancy. His body weight was 3,680 g (+1.6 SD), his height was 50.0 cm (−0.5 SD), and his head circumference (HC) was 34.0 cm (−0.5 SD). His early developmental milestones were normal with head control and reach to toys at 4 months, roll at 6 months and grasp with two fingers at 7 months. At 10 months, he was referred to our hospital because of an inability to sit. His body weight was 9,120 g (±0.0 SD), his height was 76.0 cm (+1.3 SD), and his HC was 48.0 cm (+1.4 SD). He could smile and swallow well. Bilateral strabismus was noted. No minor anomalies were noticed. Muscle tone was normal. Deep tendon reflexes were normal with negative Babinski sign. He showed athetoid movements of trunk and extremities. He showed pes equinovarus at traction response. Levels of lactate and pyruvate were normal with 12.2 and 0.89 mg/dl (L/P ratio = 13.7), respectively. Other laboratory examinations, including blood gas, blood sugar, ammonia, AST, ALT, BUN, Creatine, TSH, T3, T4, amino acids, and urine organic acid analyses were all normal. Electroencephalogram (EEG) showed no abnormalities. He was suspected to have dyskinetic cerebral palsy and referred to the division of rehabilitation. He could crawl at the age of 2. At 6 years, he experienced a loss of consciousness followed by generalized tonic–clonic convulsion with fever and was admitted to another hospital. He was diagnosed with bilateral infarction of the basal ganglia. Although EEG showed no abnormalities, clonazepam was started with the suspicion of symptomatic epilepsy. At the age of 9, he was referred to us again. His weight was 19.1 kg (−4.5 SD), his height was 115.0 cm (−2.8 SD). He lost the ability to speak several words and switched handedness from right to left. He also showed other signs of regression: including spasticity with elevated deep tendon reflexes and positive Babinski sign. In addition, he suffered bilateral hip joint dislocations and the foot deformity became worse. Contractures were noted in all extremities. Brain magnetic resonance imaging (MRI) revealed a bilateral necrotic lesion of the globus pallidus (Fig. 2a, b). EEG and motor conduction velocities were normal. Laboratory examinations, including lactate and pyruvate, were all normal. At the age of 12, he was admitted with acute bronchitis, at that time he showed an increase of blood ketone bodies: acetoacetic acid, 720 μmol/l; 3OHBA, 974 μmol/l and urine ketone (+++). Blood levels of ammonia (18 μmol/l), sugar (125 mg/dl) and lactate/pyruvate (5.1/0.29 mg/dl) were all within normal range. The values of blood ketone bodies returned to normal level with the cease of fever. Deficiencies of 3-ketothiolase and succinyl-CoA:3-oxoacid CoA transferase were ruled out by enzyme analysis using fibroblasts. His clinical symptoms and repeated MRI show the non-progressive course of his disease. Currently he is unable to sit or speak any words. Despite the addition of carbamazepine and lamotrigine, he still exhibits generalized tonic–clonic convulsion a few times a year. He also takes medicine for hypertonicity including dantrolene sodium, diazepam, baclofen and levodopa.

Patient II-3 (Fig. 1a; Table 1), the younger brother of II-2, was born uneventfully. He was born at 37 week's gestation without asphyxia after an uneventful pregnancy. His body weight was 3,668 g (+1.5 SD), his height was 50.0 cm (+0.5 SD), and his HC was 36.0 cm (−0.5 SD). He suffered from bacterial meningitis of unknown origin at 1 month of age. He became unconscious followed by convulsion and gastroenteritis at 1 year and 11 months. Brain MRI showed marked swelling of the basal ganglia (Fig. 2c, d). He was diagnosed with bilateral infarction of the basal ganglia. After this event, he became left handed. When he was 2 years old, surgery was performed to correct bilateral inner strabismus. He was referred to our hospital at the age of 4 for evaluation. His body weight was 11.0 kg (−2.2 SD), his height was 92.5 cm (−1.2 SD), and his HC was 49.5 cm (−1.3 SD). He could respond with a smile to his mother's voice. Motor milestones were delayed with no head control. No minor anomalies were noticed. Muscle tone was hypotonic. Deep tendon reflexes were exaggerated with positive Babinski sign and ankle clonus. He showed pes equinovarus. He showed a significant increase of blood acetoacetic acid of 1,270 μmol/l and 3-OHBA of 3,270 μmol/l. Levels of blood lactate and pyruvate were normal (6.2 and 0.48 mg/dl, respectively, L/P ratio = 12.9).

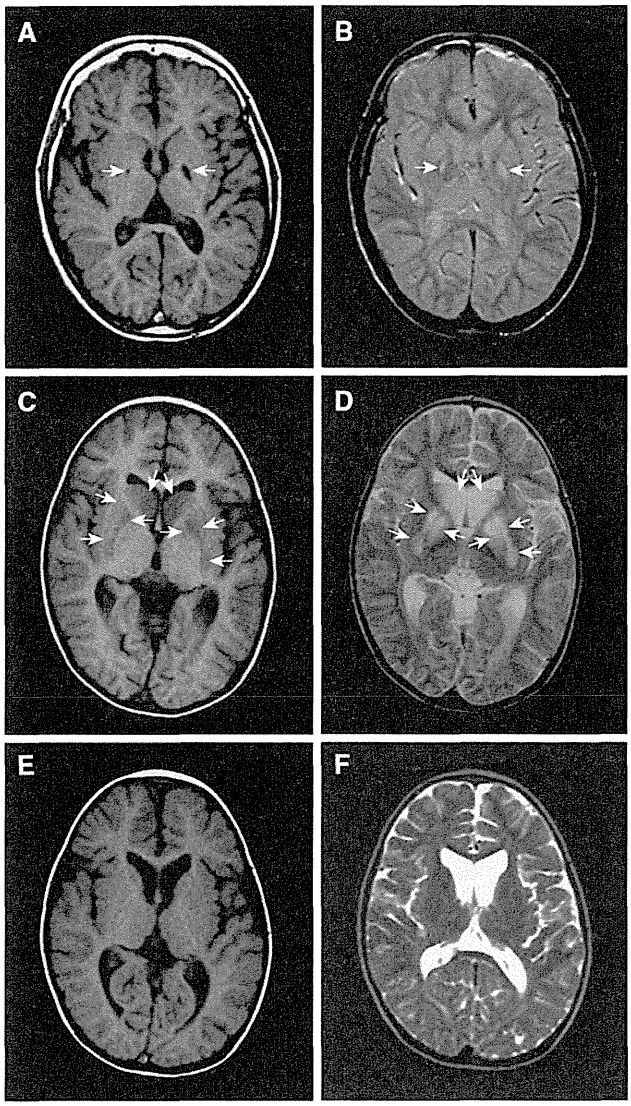

Fig. 2 Brain MRI of affected patients with a *GYG2* mutation. **a**, **b** (Patient II-2): T1 (**a**) and T2 (**b**) weighted brain magnetic resonance imaging (MRI) show necrotic lesion of bilateral globus pallidus (*arrows*). T2 elongation is observed at deep white matter at 1 year. **c–f** (Patient II-3): MRI at 1 year and 11 months shows swellings of caudate nuclei, globus pallidus, and putamen with the decreased T1 intensity (**c**) and increased T2 signals (**d**). *Arrows* indicate swollen lesions in basal ganglia. At 4 years (**e**, **f**), swelling of basal ganglia disappeared with continued mild high intensity in T2 weighted image (**f**)

Lactate and pyruvate levels of cerebrospinal fluid were slightly elevated with 11.3 and 1.11 mg/dl, respectively. Other laboratory examinations, including blood gas, blood sugar, ammonia, AST, ALT, BUN, Creatine, TSH, T3, T4, amino acids, and lysosomal enzymes were all normal. Urine organic acid analyses showed an increase of acetoacetic acid, 3-OHBA, and 3-OH-isovaleric acid. EEG showed no paroxysmal discharges. Muscle biopsy showed no specific abnormalities and no ragged red fibers. Staining for cytochrome c oxidase was normal (data not shown).

Brain MRI disclosed T2 elongation in the basal ganglia and cerebral deep white matter (Fig. 2e, f). At the age of 5, he showed lethargy with fever. At 6 years, he again showed lethargy. Biochemical analysis disclosed a significant increase of blood ketone bodies: acetoacetic acid, 1,337 μmol/l; 3-OHBA, 4,845 μmol/l and urine ketone (+++). Blood levels of ammonia (28 μmol/l), sugar (78 mg/dl), lactate (5.1 mg/dl) and pyruvate (0.43 mg/dl) were all within normal range. Blood gas analysis revealed metabolic ketoacidosis with an increase of anion gap; 22.4 mEq/l (normal range 12 ± 2). His consciousness and biochemical measurements returned to normal within a few days with intravenous fluid infusion. Similar ketoacidosis attacks were repeatedly observed and agenesis of the left kidney and neurogenic bladder were recognized at the age of 8. He started intermittent urinary catheterization, and suffered from repeated urinary tract infections, resulted in chronic renal failure. Repeated brain MRI shows the progression of cerebral and cerebellar atrophy. He is now 19 years old and shows no gain of motor or intellectual abilities from the age of 4. He takes dantrolene sodium and diazepam for hypertonicity, and spherical charcoal, allopurinol for renal failure.

Identification of a *GYG2* variant by exome sequencing

A total of 2,433,011,483 bps (II-2) and 7,926,169,749 bps (II-3) were mapped to RefSeq coding DNA sequence (CDS). 83.3 and 96.0 % of CDS were covered by ten reads and more. We used only NGS data of II-3 for selecting candidate variants as the lower-quality NGS data of II-2 may lead to erroneous conclusion. Based on the hypothesis that this syndrome is inherited in an autosomal recessive or an X-linked recessive fashion, we focused on homozygous or compound heterozygous variants on autosomes and hemizygous variants on the X chromosome. While nine variants in four candidate genes were selected by in silico flow, only one hemizygous missense mutation in *GYG2* gene agreed with the familial segregation pattern (autosomal recessive or X-linked recessive) (Table S1, S2). The c.665G>C (p.W222S) in *GYG2* (isoform a: NM_001079855) was hemizygous in affected sibs and heterozygous in their mother, consistent with the X-linked recessive model, and was confirmed by Sanger sequence (Fig. 1b). The variant was absent in our in-house Japanese exome data ($n = 418$), the 1,000 Genomes database and ESP6500. Furthermore, no pathological variants in mtDNA were detected by exome sequence (Supplementary Results, Figure S1). In addition, a total of 21 LS patients (12 males and 9 females) were screened, but no pathological changes were found in *GYG2*.

GYG2 encodes GYG2 proteins with at least five isoforms: isoform a (NM_001079855), isoform b (NM_003918),

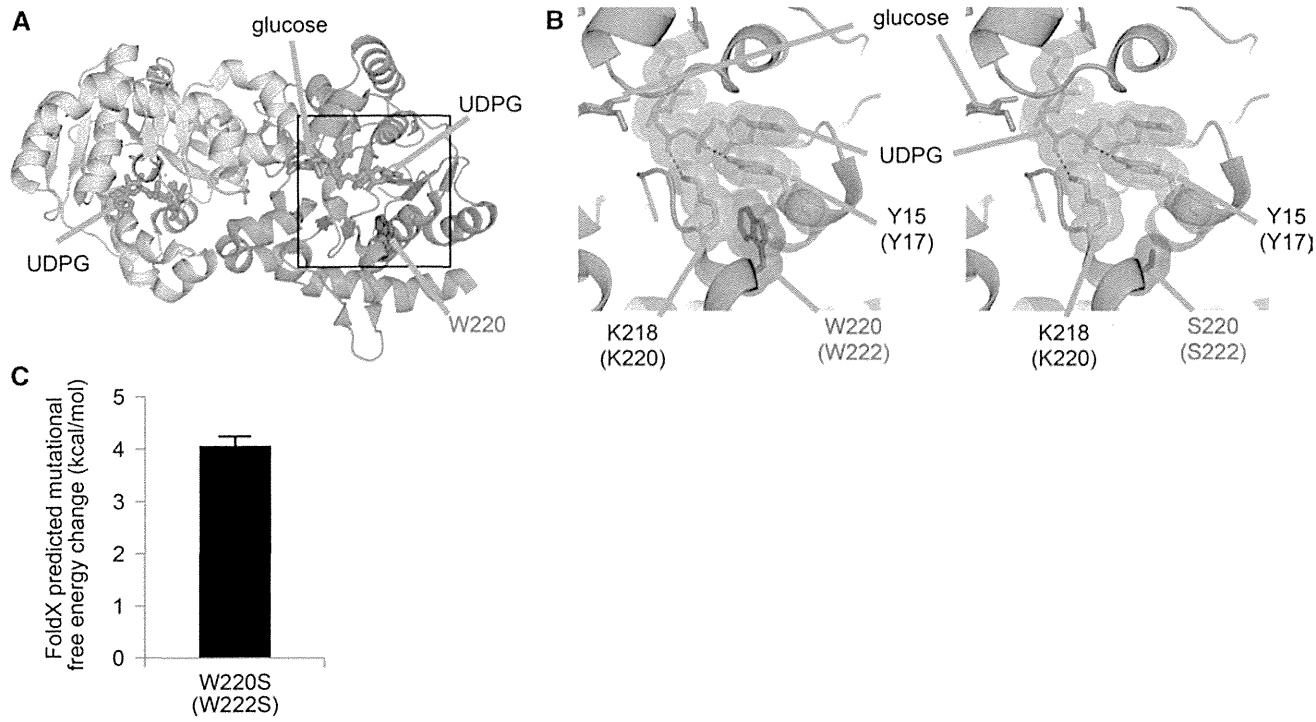

Fig. 3 Molecular structural consideration of the W222S mutation of GYG2. **a** Crystal structure of human GYG1 (Protein Data Bank code; 3T7O) (Chaikuad et al. 2011). Each monomer is colored *yellow* and *cyan*. α-helices, β-sheet and loops are drawn as *ribbons*, *arrows* and *threads*, respectively. The side chain of W222, glucose and UDP-glucose (UDPG) are shown as *sticks* in *red*, *orange* and *green*, respectively. Amino acid numbering shown is for human GYG1 with that for human GYG2 in *parenthesis*. The *squared area* corresponds to the close-up views in (**b**). **b** Detailed views of structures of the wild-type (*left*) and mutated GYG2 (p.W222S) (*right*). Amino acid residues at positions of 15, 218 and 220 and UDPG are shown as sticks with van der Waals representation and annotations. Hydrogen bonds are depicted as *dotted lines*. **c** Calculated free energy change upon the p.W222S mutation of GYG2 using FoldX software. All the molecular structures were drawn using PyMOL (www.pymol.org)

isoform c (NM_001184702), isoform d (NM_001184703), and isoform e (NM_001184704). At least two GYG2 isoforms (isoform a and b) are expressed preferentially in liver, heart and pancreas (Mu et al. 1997), while the detailed expression and function of other isoforms are undetermined. GYG2 has a glycosyltransferase family 8 domain and initiates glucose addition on its Tyrosine residue (Y197 in isoform a) via *O*-glycosylation (self-glucosylation) and can also attach an additional 7–10 residues of UDP-glucose to itself (Bollen et al. 1998; Lomako et al. 2004; Zhai et al. 2001). The W222 within the glycosyltransferase family 8 domain is evolutionarily highly conserved from *S. cerevisiae* to *H. sapiens* (Fig. 1c, d). In addition, all isoforms contain this residue. Thus, it is thought that this mutation may impair its biological function.

Structural consideration of the p.W222S mutation in human GYG2

The amino acid residue W222 of GYG2 (isoform a) was mapped to the crystal structure of human GYG1 (Chaikuad et al. 2011), since no experimental structure of GYG2 was available. W222 is involved in a hydrophobic core near the UDP-glucose (UDPG) binding site along with Y17 and K220 (Fig. 3a, b). The side chains of Y17 and K220 are hydrogen-bonded to UDPG, and the former also makes van der Waals contacts with the uridine ring of UDPG in a stacking mode. Therefore, the formation of the hydrophobic core appears to be a prerequisite for UDPG binding. To estimate the impact of the W222S mutation on the protein stability, we modeled the mutant structure and calculated the free energy change upon the mutation using the FoldX software. As a result, the mutation was predicted to destabilize the protein structure with about 4 kcal/mol increase in free energy (Fig. 3c). This suggests that the W222S mutation would impair UDPG binding (Fig. 3b).

Self-glucosylation analysis

To see the functional effects of the *GYG2* mutation in vitro, glucosyltransferase activity monitoring by self-glucosylation was measured using wild-type (WT) and W222S mutant (Mut) GYG2 (isoform a) transiently

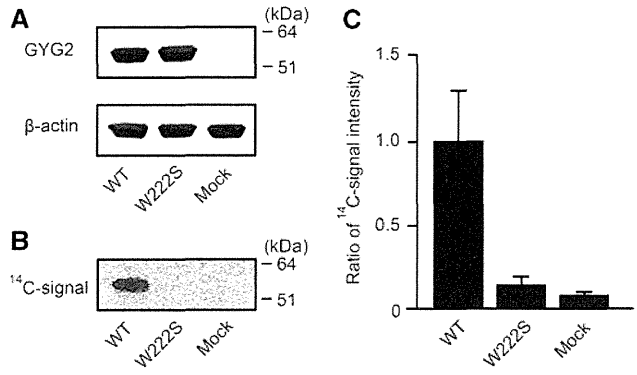

Fig. 4 Enzyme activity of GYG2. **a** Western blot analysis of recombinant GYG2. Wild-type (WT) and mutant (p.W222S) GYG2 was detected at the expected size (52 kDa). β-actin (42 kDa) was used as an internal control. **b** Autoradiography images presenting ^{14}C glucosylation toward GYG2. The signal was detected in WT, but undetected in mutant, with similar levels to Mock. **c** Graphic presentation of autoglucosylation of GYG2. The activity detected in Mock might be due to the endogenous glycogenin. *Error bars* represent the standard error of the mean

overexpressed in COS-1 cells. By immunoblotting, the expected 52 kDa bands of recombinant WT and Mut GYG2 were detected with similar expression levels (Fig. 4a). While WT GYG2 showed reasonable glucosyltransferase activity, Mut GYG2 almost completely lost the enzyme activity and was similar to the Mock level (Fig. 4b, c).

Expression analysis of GYG1 and GYG2

To observe tissue distribution of the human *GYG1* and *GYG2*, expression analysis was performed using multiple tissue cDNA panels. *GYG1* was expressed preferentially in skeletal muscle and heart from fetus to adult stages as previous reports (Barbetti et al. 1996). *GYG2* is dominantly expressed in liver from fetus through adult stages and moderately expressed in brain, heart, pancreas and kidney (Supplementary Results, Figure S2). To be marked, *GYG1* is not expressed in liver and brain where *GYG2* is highly expressed.

Discussion

In this study, we analyzed unique brothers affected with LS who were born to non-consanguineous healthy parents after uneventful pregnancies. Patient II-2 and II-3 developed LS accompanied by delayed developmental milestones at 10 months and 13 months of age, respectively. Their age of onset, clinical features and brain imaging were compatible with the diagnosis of LS. Interestingly, CNS abnormalities were observed (developmental delay, convulsion, athetoid movements, nystagmus, hypotonia, spasticity, increased deep tendon reflex and abnormal reflection), but involvement of peripheral nerve and extraneural organs was obscure. Based on the facts including (1) male (X-linked recessive), (2) normal lactate/pyruvate, (3) ketonemia/ketonuria, and (4) CNS predominant symptoms, the hemizygous *GYG2* mutation was highlighted a primary culprit.

In this study, we first identified a human *GYG2* mutation in affected brothers with LS with ketonemia/ketonuria but normal blood lactate/pyruvate. We can hypothesize a pathomechanism of the *GYG2* impairment in this family based on the canonical pathway of glycogen metabolism (Fig. 5). As glycogen storage in liver might be decreased because of the GYG2 malfunction, glucose is easily depleted. To keep appropriate blood glucose concentrations, the metabolism would be shifted toward gluconeogenesis and beta-oxidation to create glucose and energy sources like Acetyl-CoA (Garber et al. 1974; Laffel 1999; Randle et al. 1964). Excess beta-oxidation would result in overproduction of ketone bodies, consistent with the observation of ketonemia and ketonuria. However, pyruvate and lactate could be normally metabolized in gluconeogenesis and/or TCA cycle and would not accumulate in the body as seen in the majority of LS patients. Interestingly, both patients showed normal blood glucose level while showing LS manifestations which might be due to tissue energy depletion. In GYG2-deficient patients, the CNS was dominantly affected, while the effect of this abnormal metabolism was thought to extend to the entire body. This predominance could be explained by high glucose consumption as the primary energy source in brain (Amaral 2012; Magistretti and Pellerin 1999) and glycogen depletion in brain tissue level, while the blood sugar level was maintained by the other compensatory mechanism. This is similar to the muscle specific phenotypes (muscle weakness and arrhythmia) observed in patients with deficiencies of "muscle form" GYG1 in the absence of hypoglycemia (Moslemi et al. 2010). Remarkably, glycogen was less in the muscle tissue of GYG1 depleted patient (Moslemi et al. 2010). These evidences might indicate that it is not always linked between glucose level in the peripheral blood and glycogen/energy supply in tissue level while we could not show the loss of glycogen in liver or brain tissues because the materials were not available. In addition, deficiencies in two paralogous enzymes, GYG1 and GYG2, result in different human diseases suggesting they are unable to compensate each other in specific organs.

The *GYG2* mutation is probably causative for LS in this family. However, it is possible that the mutation is just coincidence because we just showed genetic evidences (due

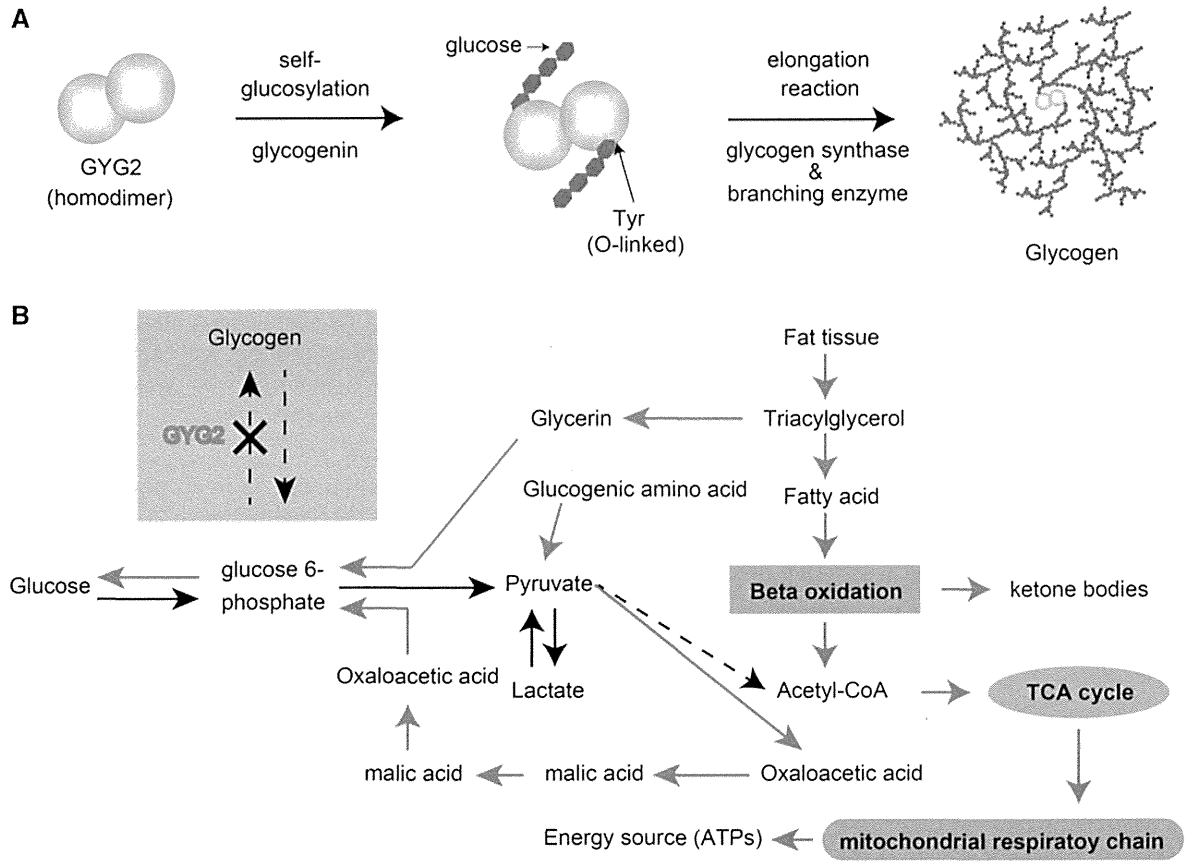

Fig. 5 Biochemical metabolisms in glycogen storage and glycolysis pathways. **a** Schematic presentation of glycogen biosynthesis. GYG2 has a catalytic capability for *O*-linked self-glucosylation at Tyrosine (Y197 in isoform a) and adds approximately 10 glucose molecules. By the subsequent elongating reactions by glycogen synthase and branching enzyme, giant molecule "glycogen" is formed. **b** Modeled biochemical pathway in GYG2 impairment. As the GYG2 impairment results in the absence of glycogen storage, glycogen is easy to be depleted and gluconeogenesis is induced from fat tissues and glucogenic amino acids. The reactions in mitochondria are shown in *yellow shadow*. While increased acetyl-CoA inhibits the pyruvate dehydrogenase complex which irreversibly converts pyruvate to acetyl-CoA (as shown as *dotted line*), it accelerates gluconeogenesis through pyruvate–oxaloacetic acid–malic acid–oxaloacetic acid. Triacylglycerol was metabolized into glycerin and fatty acid. Fatty acid was used for beta-oxidation and ketone production. The *arrows* indicate the directions of normal metabolism. *Red arrows* indicate the predicted predominant pathways in GYG2-deficient patients

to its rarity and familial co-segregation) and GYG2 loss of function by in vitro study without showing any sufficient data on how the *GYG2* mutation causes LS.

In conclusion, we describe the first human variant of *GYG2* which may be associated with the atypical LS phenotype in this family. Further studies are absolutely needed to conclude whether *GYG2* abnormality leads to atypical LS observed in this family.

Acknowledgments We thank all the patients and their families for participating in this work. We deeply appreciate Dr. Toshiyuki Fukao, who is the professor of Department of Pediatrics, Graduate School of Medicine, Gifu University, for the enzyme assay for 3-ketothiolase deficiency and succinyl-CoA:3-oxoacid CoA transferase. We would like to thank Dr. Yasushi Okazaki at Research Center for Genomic Medicine, Saitama Medical University for helpful discussion. We also thank Ms. Y. Yamashita, S. Sugimoto and K. Takabe for their technical assistance. This work was supported by research grants from the Ministry of Health, Labour, and Welfare (H. Saitsu, N. Matsumoto and N. Miyake), the Japan Science and Technology Agency (N. Matsumoto), the Strategic Research Program for Brain Sciences (to N. Matsumoto), a Grant-in-Aid for Scientific Research on Innovative Areas (Transcription Cycle) from the Ministry of Education, Culture, Sports, Science, and Technology of Japan (N. Matsumoto), a Grant-in-Aid for Scientific Research from the Japan Society for the Promotion of Science (to N. Matsumoto), a Grant-in-Aid for Young Scientists from the Japan Society for the Promotion of Science (H. Saitsu and N. Miyake), a grant from the 2012 Strategic Research Promotion of Yokohama City University (N. Matsumoto), and research grants from the Japan Epilepsy Research Foundation (H. Saitsu) and the Takeda Science Foundation (N. Matsumoto and N. Miyake).

Conflict of interest The authors declare that they have no conflict of interest.

References

Amaral AI (2012) Effects of hypoglycaemia on neuronal metabolism in the adult brain: role of alternative substrates to glucose. J Inherit Metab Dis. doi:10.1007/s10545-012-9553-3

Antonicka H, Ostergaard E, Sasarman F, Weraarpachai W, Wibrand F, Pedersen AM, Rodenburg RJ, van der Knaap MS, Smeitink JA, Chrzanowska-Lightowlers ZM, Shoubridge EA (2010) Mutations in C12orf65 in patients with encephalomyopathy and a mitochondrial translation defect. Am J Hum Genet 87:115–122. doi:10.1016/j.ajhg.2010.06.004

Barbetti F, Rocchi M, Bossolasco M, Cordera R, Sbraccia P, Finelli P, Consalez GG (1996) The human skeletal muscle glycogenin gene: cDNA, tissue expression and chromosomal localization. Biochem Biophys Res Commun 220:72–77. doi:10.1006/bbrc 1996.0359

Benke PJ, Parker JC Jr, Lubs ML, Benkendorf J, Feuer AE (1982) X-linked Leigh's syndrome. Hum Genet 62:52–59

Bollen M, Keppens S, Stalmans W (1998) Specific features of glycogen metabolism in the liver. Biochem J 336:19–31

Brown GK, Squier MV (1996) Neuropathology and pathogenesis of mitochondrial diseases. J Inherit Metab Dis 19:553–572

Cao Y, Mahrenholz AM, DePaoli-Roach AA, Roach PJ (1993) Characterization of rabbit skeletal muscle glycogenin. Tyrosine 194 is essential for function. J Biol Chem 268:14687–14693

Chaikuad A, Froese DS, Berridge G, von Delft F, Oppermann U, Yue WW (2011) Conformational plasticity of glycogenin and its maltosaccharide substrate during glycogen biogenesis. Proc Natl Acad Sci USA 108:21028–21033. doi:10.1073/pnas.1113921108

Debray FG, Morin C, Janvier A, Villeneuve J, Maranda B, Laframboise R, Lacroix J, Decarie JC, Robitaille Y, Lambert M, Robinson BH, Mitchell GA (2011) LRPPRC mutations cause a phenotypically distinct form of Leigh syndrome with cytochrome c oxidase deficiency. J Med Genet 48:183–189. doi:10.1136/jmg.2010.081976

Farina L, Chiapparini L, Uziel G, Bugiani M, Zeviani M, Savoiardo M (2002) MR findings in Leigh syndrome with COX deficiency and SURF-1 mutations. AJNR Am J Neuroradiol 23:1095–1100

Finsterer J (2008) Leigh and Leigh-like syndrome in children and adults. Pediatr Neurol 39:223–235. doi:10.1016/j.pediatrneurol.2008.07.013

Garber AJ, Menzel PH, Boden G, Owen OE (1974) Hepatic ketogenesis and gluconeogenesis in humans. J Clin Invest 54:981–989. doi:10.1172/JCI107839

Gibbons BJ, Roach PJ, Hurley TD (2002) Crystal structure of the autocatalytic initiator of glycogen biosynthesis, glycogenin. J Mol Biol 319:463–477. doi:10.1016/S0022-2836(02)00305-4

Guerois R, Nielsen JE, Serrano L (2002) Predicting changes in the stability of proteins and protein complexes: a study of more than 1000 mutations. J Mol Biol 320:369–387. doi:10.1016/S0022-2836(02)00442-4

Khan S, Vihinen M (2010) Performance of protein stability predictors. Hum Mutat 31:675–684. doi:10.1002/humu.21242

Krisman CR, Barengo R (1975) A precursor of glycogen biosynthesis: alpha-1,4-glucan-protein. Eur J Biochem 52:117–123

Laffel L (1999) Ketone bodies: a review of physiology, pathophysiology and application of monitoring to diabetes. Diabetes Metab Res Rev 15:412–426

Larner J (1953) The action of branching enzymes on outer chains of glycogen. J Biol Chem 202:491–503

Leigh D (1951) Subacute necrotizing encephalomyelopathy in an infant. J Neurol Neurosurg Psychiatry 14:216–221

Lomako J, Lomako WM, Whelan WJ (1988) A self-glucosylating protein is the primer for rabbit muscle glycogen biosynthesis. FASEB J 2:3097–3103

Lomako J, Lomako WM, Whelan WJ (2004) Glycogenin: the primer for mammalian and yeast glycogen synthesis. Biochim Biophys Acta 1673:45–55. doi:10.1016/j.bbagen.2004.03.017

Lopez LC, Schuelke M, Quinzii CM, Kanki T, Rodenburg RJ, Naini A, Dimauro S, Hirano M (2006) Leigh syndrome with nephropathy and CoQ10 deficiency due to decaprenyl diphosphate synthase subunit 2 (PDSS2) mutations. Am J Hum Genet 79:1125–1129. doi:10.1086/510023

Magistretti PJ, Pellerin L (1999) Cellular mechanisms of brain energy metabolism and their relevance to functional brain imaging. Philos Trans R Soc Lond B Biol Sci 354:1155–1163. doi:10.1098/rstb 1999.0471

Martin MA, Blazquez A, Gutierrez-Solana LG, Fernandez-Moreira D, Briones P, Andreu AL, Garesse R, Campos Y, Arenas J (2005) Leigh syndrome associated with mitochondrial complex I deficiency due to a novel mutation in the NDUFS1 gene. Arch Neurol 62:659–661. doi:10.1001/archneur.62.4.659

Medina L, Chi TL, DeVivo DC, Hilal SK (1990) MR findings in patients with subacute necrotizing encephalomyelopathy (Leigh syndrome): correlation with biochemical defect. AJR Am J Roentgenol 154:1269–1274

Moslemi AR, Lindberg C, Nilsson J, Tajsharghi H, Andersson B, Oldfors A (2010) Glycogenin-1 deficiency and inactivated priming of glycogen synthesis. N Engl J Med 362:1203–1210. doi:10.1056/NEJMoa0900661

Mu J, Roach PJ (1998) Characterization of human glycogenin-2, a self-glucosylating initiator of liver glycogen metabolism. J Biol Chem 273:34850–34856

Mu J, Skurat AV, Roach PJ (1997) Glycogenin-2, a novel self-glucosylating protein involved in liver glycogen biosynthesis. J Biol Chem 272:27589–27597

Naess K, Freyer C, Bruhn H, Wibom R, Malm G, Nennesmo I, von Dobeln U, Larsson NG (2009) MtDNA mutations are a common cause of severe disease phenotypes in children with Leigh syndrome. Biochim Biophys Acta 1787:484–490. doi:10.1016/j.bbabio.2008.11.014

Ostergaard E, Hansen FJ, Sorensen N, Duno M, Vissing J, Larsen PL, Faeroe O, Thorgrimsson S, Wibrand F, Christensen E, Schwartz M (2007) Mitochondrial encephalomyopathy with elevated methylmalonic acid is caused by SUCLA2 mutations. Brain 130:853–861. doi:10.1093/brain/awl383

Picardi E, Pesole G (2012) Mitochondrial genomes gleaned from human whole-exome sequencing. Nat Methods 9:523–524. doi:10.1038/nmeth.2029

Pitcher J, Smythe C, Cohen P (1988) Glycogenin is the priming glucosyltransferase required for the initiation of glycogen biogenesis in rabbit skeletal muscle. Eur J Biochem 176:391–395

Quinonez SC, Leber SM, Martin DM, Thoene JG, Bedoyan JK (2013) Leigh syndrome in a girl with a novel DLD mutation causing E3 deficiency. Pediatr Neurol 48:67–72. doi:10.1016/j.pediatrneurol.2012.09.013

Rahman S, Blok RB, Dahl HH, Danks DM, Kirby DM, Chow CW, Christodoulou J, Thorburn DR (1996) Leigh syndrome: clinical features and biochemical and DNA abnormalities. Ann Neurol 39:343–351. doi:10.1002/ana.410390311

Randle PJ, Newsholme EA, Garland PB (1964) Regulation of glucose uptake by muscle. 8. Effects of fatty acids, ketone bodies and pyruvate, and of alloxan-diabetes and starvation, on the uptake and metabolic fate of glucose in rat heart and diaphragm muscles. Biochem J 93:652–665

Smythe C, Caudwell FB, Ferguson M, Cohen P (1988) Isolation and structural analysis of a peptide containing the novel tyrosyl-glucose linkage in glycogenin. EMBO J 7:2681–2686

van Erven PM, Cillessen JP, Eekhoff EM, Gabreels FJ, Doesburg WH, Lemmens WA, Slooff JL, Renier WO, Ruitenbeek W (1987)

Leigh syndrome, a mitochondrial encephalo(myo)pathy. A review of the literature. Clin Neurol Neurosurg 89:217–230

Viskupic E, Cao Y, Zhang W, Cheng C, DePaoli-Roach AA, Roach PJ (1992) Rabbit skeletal muscle glycogenin. Molecular cloning and production of fully functional protein in Escherichia coli. J Biol Chem 267:25759–25763

Zhai L, Schroeder J, Skurat AV, Roach PJ (2001) Do rodents have a gene encoding glycogenin-2, the liver isoform of the self-glucosylating initiator of glycogen synthesis? IUBMB Life 51:87–91. doi:10.1080/15216540117315

ELSEVIER

Brain & Development 36 (2014) 730–733

BRAIN & DEVELOPMENT
Official Journal of the Japanese Society of Child Neurology

www.elsevier.com/locate/braindev

Case report

Leigh syndrome with Fukuyama congenital muscular dystrophy: A case report

Hidehito Kondo [a,b,*], Koichi Tanda [a], Chihiro Tabata [a], Kohei Hayashi [a], Minako Kihara [a], Zenro Kizaki [a], Mariko Taniguchi-Ikeda [c], Masato Mori [d], Kei Murayama [e], Akira Ohtake [f]

[a] *Department of Pediatrics and Neonatology, Japanese Red Cross Kyoto Daiichi Hospital, Japan*
[b] *Department of Pediatrics, Osaka University Graduate School of Medicine, Japan*
[c] *Division of Pediatrics, Kobe University Graduate School of Medicine, Japan*
[d] *Department of Pediatrics, Jichi Medical University, Japan*
[e] *Department of Metabolism, Chiba Children's Hospital, Japan*
[f] *Department of Pediatrics, Saitama Medical University Hospital, Japan*

Received 20 January 2013; received in revised form 2 September 2013; accepted 13 September 2013

Abstract

We report the first case of Leigh syndrome (LS) with Fukuyama congenital muscular dystrophy (FCMD). A neonate suffered from lactic acidosis and subsequently presented with poor feeding, muscle weakness, hypotonia, cardiopulmonary dysfunction, and hydrocephalus. He died at 17 months. The findings of brain magnetic resonance imaging indicated some specific features of both LS and FCMD, and FCMD gene mutation was detected. Decreased mitochondrial respiratory complex I and II activity was noted. Mitochondrial DNA sequencing showed no pathogenic mutation. A case with complex I + II deficiency has rarely been reported, suggesting a nuclear gene mutation.

Keywords: Leigh syndrome; FCMD; Mitochondria; Complex I + II deficiency

1. Introduction

Fukuyama congenital muscular dystrophy (FCMD), one of the most common autosomal recessive disorders in the Japanese population, is characterized by congenital muscular dystrophy with cortical dysgenesis. The gene responsible for FCMD is located on 9q31. Most FCMD-bearing chromosomes (87%) have a 3-kb retrotransposal insertion in the 3′-untranslated region of the gene [1].

Leigh syndrome (LS) is a progressive neurodegenerative disorder with psychomotor retardation, signs and symptoms of brain stem and/or basal ganglia involvement, and raised lactate levels in blood and/or cerebrospinal fluid (CSF). In majority of the cases, dysfunction of the mitochondrial respiratory chain is responsible for the disease. LS is caused by either mitochondrial or nuclear gene mutations with large genetic heterogeneity [2]. Here, we report the first case of LS with FCMD.

2. Case report

2.1. Index case

A Japanese boy was born at term as the third child to non-consanguineous healthy parents. His serum creatine

* Corresponding author at: Department of Pediatrics, Osaka University Graduate School of Medicine, 2-2 Yamadaoka, Suita City, Osaka 565-0871, Japan. Tel.: +81 6 6879 3932; fax: +81 6 6879 3939.
E-mail address: hkondo@ped.med.osaka-u.ac.jp (H. Kondo).

0387-7604/$ - see front matter © 2013 The Japanese Society of Child Neurology. Published by Elsevier B.V. All rights reserved.
http://dx.doi.org/10.1016/j.braindev.2013.09.005

kinase concentration was extremely high (45149 IU/L) on the day of birth without any anomaly. Serum lactate level, plasma amino acid profiles, and carnitine profiles were normal. Urinary organic acid profiles showed no specific abnormalities. The patient suddenly suffered from severe lactic acidosis, hyperglycemia, and acute heart failure at day 17. Levels of lactate and pyruvate in the CSF were 4.9 mM and 0.21 mM. A mitochondrial disorder was suspected and treatment was started with carnitine, ubiquinone, and other vitamins in addition to cardiotonics and insulin. The infant's condition improved, but he subsequently presented with poor feeding, muscle weakness, and hypotonia at 1 month. Hypertrophic cardiomyopathy occurred at 3 months and cardiopulmonary function worsened after repeated lactic acidosis, and he required mechanical ventilation from the age of 6 months. He presented with an enlarged head circumference and a tense anterior fontanelle at 12 months, and died of pneumonia at 17 months.

Magnetic resonance imaging (MRI)at 2 months revealed cerebellar cysts, pachygyria, and T2-hyperintense lesions in white matter and the brainstem, but basal ganglia were normal (Fig. 1A). A follow-up investigation at 4 months indicated extended T2-hyperintense lesions (Fig. 1B). A brain computed tomography (CT) scan at 14 months showed severe hydrocephalus and extensive cerebral atrophy (Fig. 1C).

Cerebellar cysts and pachygyria are characteristic of FCMD, genetic testing for *FCMD* was performed. We examined retrotransposal insertion into the 3′-untranslated region (UTR) of the *FCMD* gene using a polymerase chain reaction (PCR)-based diagnostic method involving peripheral blood leukocytes of this case and his parents [1]. A homozygous mutation of this case and heterozygous mutation of his parents were detected. Repeated lactic acidosis and brain stem lesions led us to suspect LS. A skin biopsy was performed for mitochondrial analysis at 1 month. Activities of mitochondrial respiratory chain complex (Co) I, II, III, and IV were assayed from skin fibroblasts, as described previously [3]. The activities were also calculated as the percent relative to citrate synthetase (CS), a mitochondrial enzyme marker and to Co II activity, and evaluated according to the diagnostic criteria [4]. Respiratory chain complex I and II activities were very low, but CS, Co III, and Co IV activities were normal (Table 1). Expression of the mitochondrial respiratory chain CoI, II, III, and IV proteins was concurrently examined by Western blotting

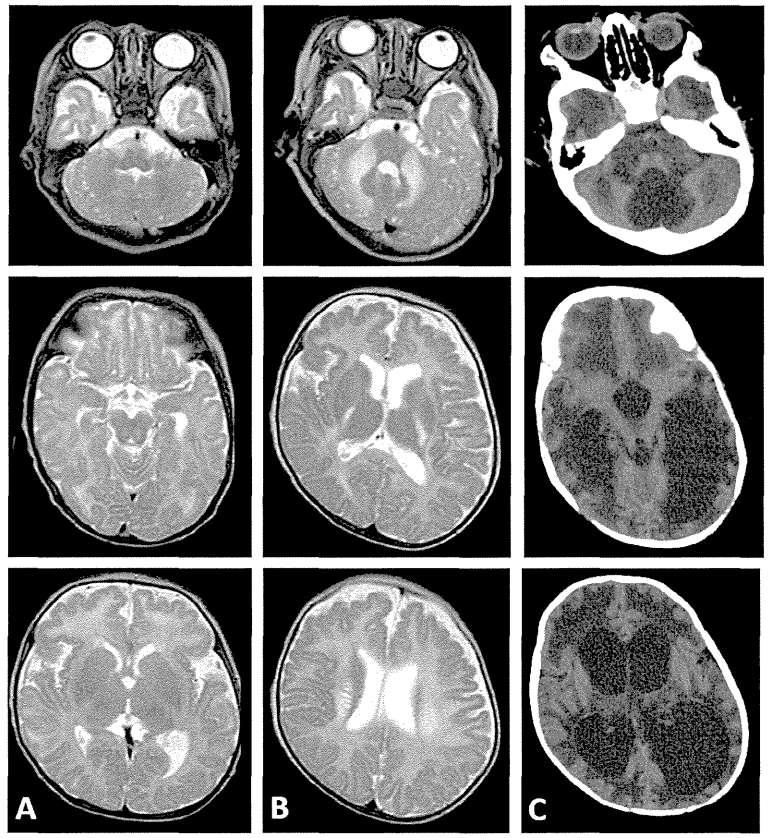

Fig. 1. Magnetic resonance image (MRI) at the age of 2 months (A) shows cerebellar cysts (A, top), bilateral symmetrical lesions in the brainstem (A, middle), pachygyria, and T2-hyperintensity in white matter, predominantly in the frontal lobes (A, bottom). An MRI at 4 months of age indicated T2-hyperintensity extending into the middle cerebellar peduncles, posterior limb of the internal capsule, and the corona radiata (B). A brain computed tomography scan at 14 months of age showed severe hydrocephalus, widespread hypodensity of white matter, and extensive cerebral atrophy (C).

Table 1
Activities of mitochondrial respiratory chain complex (Co) I, II, III, and IV; citrate synthase (CS) from skin fibroblasts. Enzyme activities are expressed as a percentage of mean relative activity of 35 normal controls and relative to CS and Co II.

	Co I	Co II	Co II + III	Co III	Co IV	CS
Crude activity (%)	32	18	21	56	45	80
CS ratio (%)	38	21	24	65	55	
Co II ratio (%)	177		112	312	259	

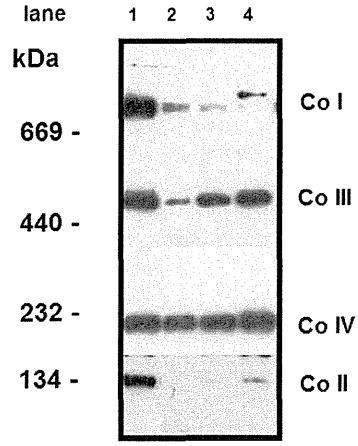

Fig. 2. Blue native polyacrylamide gel electrophoresis (BN-PAGE) analysis of skin fibroblasts 1: control; 2: this case; 3: a double of lane 2; 4: a triple of lane 2. The bands corresponding to Co II were almost invisible and those corresponding to Co I were markedly weak, whereas the intensities of the Co III and IV bands gradually became strong.

using blue native polyacrylamide gel electrophoresis (BN-PAGE), as described previously [5]. The BN-PAGE analysis showed that the bands corresponding to Co II were almost invisible and those corresponding to Co I were markedly weak (Fig. 2). This finding was in agreement with the enzyme activity assay results. The mitoSEQr™ system (Applied Biosystems, Foster City, CA, USA) was used for the entire mitochondrial DNA analysis. Genomic DNA was extracted from skin fibroblasts. Data were analyzed with SeqScape Software v2.5 and compared with mitochondrial DNA sequences (Mitomap: www.mitomap.org). Several base substitutions were detected, but no pathogenic mutation was detected in the entire mitochondrial DNA sequence. High resolution chromosome analysis was normal.

2.2. Family history

The index case's older brother had repeated afebrile convulsions since the age of 2 months, but brain MRI findings were normal. Laboratory tests showed elevated level of lactate (2.92 mM) in CSF and a normal level of serum creatine kinase (75 IU/L). He died of sudden cardiac dysfunction at 4 months. The second child was a healthy girl with normal development.

3. Discussion

A case of FCMD and mitochondrial respiratory chain disorder (MRCD) has never been reported. The pathophysiology of FCMD and MRCD is quite different, therefore, low activities of the respiratory chain complexes in this case were probably not due to FCMD. LS is clinically characterized by a wide variety of manifestations involving multiple organs in infancy or early childhood. Thus, the early onset of his symptoms suggested that LS was the main cause.

White matter abnormalities in patients with FCMD are often detected by MRI as transient T2-hyperintensity. Kato et al. reported that the pathological origin of white matter lesions is dysmyelination and that the lesions are masked by brain development [6]. In this case, the extended signal abnormalities had different features compared with those of FCMD. Some cases of complex II deficiency with extensive T2-hyperintensities in white matter have been reported [7,8]. The white matter abnormalities in our case may have been associated with the complex II deficiency. The patient presented with progressive hydrocephalus, but he had no prior clinical signs of intraventricular hemorrhage or infection in CSF. Patients with FCMD, who are homozygotes for the insertion mutation with hydrocephalus have never been reported [9]. A few patients with LS develop cerebellar atrophy or ventricular enlargement [10].

Many cases of combined complex deficiencies have been reported, but a case with a complex I + II deficiency has rarely been reported. The entire mitochondrial DNA sequencing in this case showed no pathogenic mutation. These findings suggest that LS in this case was the result of a nuclear gene mutation.

The genes responsible for mitochondrial disease located contiguous to the FCMD gene have not been identified. The infant's older brother was suspected to have MRCD without obvious clinical signs of FCMD. Therefore, we speculated that the present case was unlikely to be a contiguous gene syndrome. We are investigating this patient's fibroblasts using next-generation sequencing to identify the causative nuclear gene mutation and the relation between the two diseases.

Potential conflict of interest report

The authors indicated no potential conflict of interest.

Acknowledgments

This study was supported, in part, by an Innovative Cell Biology grant from Innovative Technology (Cell Innovation Program) of the Ministry of Education, Culture, Sports, Science, and Technology, Japan. Our work

was also supported by grants-in-aid of the research on intractable diseases (mitochondrial disorders) of the Ministry of Health, Labour and Welfare of Japan.

References

[1] Watanabe M, Kobayashi K, Jin F, Park K, Yamada T, Tokunaga K, et al. Founder SVA retrotransposal insertion in Fukuyama-type congenital muscular dystrophy and its origin in Japanese and Northeast Asian populations. Am J Med Genet A 2005;138:344–8.

[2] Finsterer J. Leigh and Leigh-like syndrome in children and adults. Pediatr Neurol 2008;39:223–35.

[3] Kirby DM, Crawford M, Cleary MA, Dennett X, Thorburn DR. Respiratory chain complex I deficiency: an under diagnosed energy generation disorder. Neurology 1999;52:1255–64.

[4] Bernier FP, Boneh A, Dennett X, Chow CW, Cleary MA, Thorburn DR. Diagnostic criteria for respiratory chain disorders in adults and children. Neurology 2002;59:1406–11.

[5] Van Coster R, Smet J, George E, De Meirleir L, Seneca S, Van Hove J, et al. Blue native polyacrylamide gel electrophoresis: a powerful tool in diagnosis of oxidative phosphorylation defects. Pediatr Res 2001;50:658–65.

[6] Kato T, Funahashi M, Matsui A, Takashima S, Suzuki Y. MRI of disseminated developmental dysmyelination in Fukuyama type of CMD. Pediatr Neurol 2000;23:385–8.

[7] Burgeois M, Goutieres F, Chretien D, Rustin P, Munnich A, Aicardi J. Deficiency in complex II of the respiratory chain, presenting as a leukodystrophy in two sisters with Leigh syndrome. Brain Dev 1992;14:404–8.

[8] Brockmann K, Bjornstad A, Dechent P, Korenke CG, Smeitink J, Trijbels J, et al. Succinate in dystrophic white matter: a proton magnetic resonance spectroscopy finding characteristic for complex II deficiency. Ann Neurol 2002;52:38–46.

[9] Saito K, Osawa M, Wang ZP, Ikeya K, Fukuyama Y, Kondo-Iida E, et al. Haplotype–phenotype correlation in Fukuyama congenital muscular dystrophy. Am J Med Genet 2000;92:184–90.

[10] Horváth R, Abicht A, Holinski-Feder E, Laner A, Gempel K, Prokisch H, et al. Leigh syndrome caused by mutations in the flavoprotein (Fp) subunit of succinate dehydrogenase (SDHA). J Neurol Neurosurg Psychiatry 2006;77:74–6.

PEDIATRICS INTERNATIONAL Official Journal of the Japan Pediatric Society

Pediatrics International (2014) **56**, 180–187 doi: 10.1111/ped.12249

Original Article

Molecular diagnosis of mitochondrial respiratory chain disorders in Japan: Focusing on mitochondrial DNA depletion syndrome

Taro Yamazaki,[1,6] Kei Murayama,[3] Alison G Compton,[6] Canny Sugiana,[6]* Hiroko Harashima,[1] Shin Amemiya,[1] Masami Ajima,[3] Tomoko Tsuruoka,[3] Ayako Fujinami,[3] Emi Kawachi,[3] Yoshiko Kurashige,[4] Kenshi Matsushita,[4] Hiroshi Wakiguchi,[4] Masato Mori,[5] Hiroyasu Iwasa,[2] Yasushi Okazaki,[2] David R Thorburn[6] and Akira Ohtake[1]

[1]*Department of Pediatrics, Faculty of Medicine and* [2]*Translational Research Center, International Medical Center, Saitama Medical University, Saitama,* [3]*Department of Metabolism, Chiba Children's Hospital, Chiba,* [4]*Department of Pediatrics, Kochi Medical School Kochi University, Kochi,* [5]*Department of Pediatrics, Jichi Medical University, Tochigi, Japan and* [6]*Murdoch Childrens Research Institute, Royal Children's Hospital and Department of Paediatrics, University of Melbourne, Melbourne, Victoria, Australia*

Abstract ***Background***: Although mitochondrial respiratory chain disorders (MRCD) are one of the most common congenital metabolic diseases, there is no cumulative data on enzymatic diagnosis and clinical manifestation for MRCD in Japan and Asia.

Methods: We evaluated 675 Japanese patients having profound lactic acidemia, or patients having symptoms or signs of multiple-organ origin simultaneously without lactic acidemia on respiratory chain enzyme activity assay and blue native polyacrylamide gel electrophoresis. Quantitative polymerase chain reaction was used to diagnose mitochondrial DNA depletion syndrome (MTDPS). Mutation analysis of several genes responsible for MTDPS was also performed.

Results: A total of 232 patients were diagnosed with a probable or definite MRCD. MRCD are common, afflicting one in every several thousand people in Japan. More than one in 10 of the patients diagnosed lacked lactic acidemia. A subsequent analysis of the causative genes of MTDPS identified novel mutations in six of the patients. A 335 bp deletion in deoxyguanosine kinase (*DGUOK*; g.11692_12026del335 (p.A48fsX90)) was noted in two unrelated families, and may therefore be a common mutation in Japanese people. The proportion of all patients with MTDPS, and particularly those with recessive *DNA polymerase γ* (*POLG*) mutations, appears to be lower in Japan than in other studies. This is most likely due to the relatively high prevalence of ancient European *POLG* mutations in Caucasian populations. No other significant differences were identified in a comparison of the enzymatic diagnoses, disease classifications or prognoses in Japanese and Caucasian patients with MRCD.

Conclusion: MTDPS and other MRCD are common, but serious, diseases that occur across all races.

Key words *DGUOK* deletion mutation, enzymatic diagnosis, mitochondrial DNA depletion syndrome, mitochondrial respiratory chain disorder, racial difference.

Mitochondrial respiratory chain disorders (MRCD) are disorders of the oxidative phosphorylation system, which is responsible for ATP production. MRCD are the most common congenital metabolic diseases, afflicting at least 1 in 5000 persons.[1] Mitochondrial DNA depletion syndrome (MTDPS), in which mitochondrial DNA (mtDNA) level is lower than normal, is one of the major MRCD. A number of responsible genes of MTDPS have been identified, and the pathophysiology of this disease is partially characterized at the molecular level.[2–5] We have previously diagnosed and characterized MRCD cases in Japan using respiratory chain enzyme analysis.[6–9] Having recently analyzed the molecular diagnoses and clinical manifestations of MRCD in Japanese patients, and analyzing several genes responsible for hepatocerebral MTDPS, we herein discuss and compare the collected data to those reported for MRCD outside of Japan.

Correspondence: Akira Ohtake, MD PhD, Department of Pediatrics, Faculty of Medicine, Saitama Medical University, 38 Morohongo, Moroyama, Iruma-gun, Saitama 350-0495, Japan. Email: akira_oh@saitama-med.ac.jp

*Present address: Monash IVF PTY Ltd, Melbourne, Victoria, Australia.

Received 11 July 2013; revised 19 August 2013; accepted 21 October 2013.

Methods

Patients and samples

The subjects consisted of patients clinically suspected of having MRCD. We measured respiratory chain enzyme activity and quantity for patients with profound lactic acidemia, or patients with symptoms or signs of multiple-organ origin simultaneously without lactic acidemia. Other metabolic disorders were excluded on plasma tandem mass spectrometry and urine organic acid analysis. Approximately half of candidates were <1 year old,